Journal of Inflammation Research Dovepress

Open Access Full Text Article ORIGINAL RESEARCH

Arctiin Alleviates Atopic Dermatitis Against Inflammation and Pyroptosis Through Suppressing TLR4/MyD88/NF-κB and NLRP3/Caspase-1/GSDMD Signaling Pathways

Jingmin Li[1,2], Xuefei Du[1], Zhenzhen Mu[1], Xiuping Han[1]

[1]Department of Dermatology, Shengjing Hospital, China Medical University, Shenyang, Liaoning, People's Republic of China; [2]Department of Dermatology, Third Hospital of Shanxi Medical University, Shanxi Bethune Hospital, Tongji Shanxi Hospital, Taiyuan, People's Republic of China

Correspondence: Xiuping Han, Department of Dermatology, Shengjing Hospital, China Medical University, Shenyang, People's Republic of China, Tel + 86 18940251646, Email hanxiuping66@126.com

Purpose: Atopic dermatitis (AD) is a prevalent skin condition worldwide. The immune response plays a crucial role in the pathogenesis of AD. Arctiin (ARC), a natural lignan, has been extensively investigated because of its anti-inflammatory, antioxidant, and anticancer properties. However, the impact of ARC on AD remains uncertain. Therefore, this study investigated the therapeutic effects of ARC in AD.

Methods: AD-like lesions were induced in mice by applying 2,4-dinitrochlorobenzene (DNCB). The efficacy of ARC in AD was assessed by measuring skin lesion scores and thickness, pathological observation, and serum IgE concentrations. The expression of relevant proteins and genes in the back skin of the mice was assessed. Moreover, the TLR4/MyD88/NF-κB and NLRP3/Caspase-1/GSDMD signaling pathways were assessed in HaCaT cells stimulated with TNF-α and IFN-γ.

Results: ARC effectively alleviated AD-like dermatitis induced by DNCB in mice, reducing the skin thickness, mast cell infiltration in skin tissue, and serum total IgE levels. In addition, the expression of IL-1β and the mRNA transcription of TSLP and IFN-γ were downregulated. ARC also suppressed the TLR4/MyD88/NF-κB pathway, and molecular docking confirmed that ARC had exceptional binding properties with TLR4. Moreover, ARC ameliorated pyroptosis by inhibiting the activation of the nod-like receptor protein-3/Caspase-1/GSDMD cascade.

Conclusion: ARC has remarkable anti-AD effects by inhibiting inflammation and pyroptosis through the TLR4/MyD88/NF-κB and NLRP3/Caspase-1/GSDMD signaling pathways. This suggests that ARC has potential as a new drug candidate for treating AD, which provides a novel approach to the clinical management of AD.

Keywords: arctiin, atopic dermatitis, inflammation, pyroptosis

Introduction

Atopic dermatitis (AD) is one of the most common chronic inflammatory cutaneous diseases, with an incidence of up to 3% in adults and 20% in children, and it affects people of all ages and ethnicities.[1] Furthermore, the prevalence of AD demonstrates an increasing trend globally.[2] AD is characterized by intense itching, approximately 91% of AD patients suffer from chronic pruritus (duration ≥ 6 weeks).[3] The patient's sleep is often disturbed, which results in a severe impairment in their overall quality of life. Moreover, AD ranks first in the global disease burden caused by skin diseases.[4] However, the pathogenesis of AD is not fully understood, which is complex and involves a strong genetic predisposition, epidermal dysfunction, and multiple immune pathways dominated by T-cell inflammation.[2] The treatment of AD involves topical agents, including corticosteroids and calcineurin inhibitors, which have remained the primary therapy options for decades.[5] However, long-term use may cause a series of side effects, such as localized skin atrophy because of corticosteroids and long-term cancer risk induced by topical calcineurin inhibitors.[6] Dupilumab targeting the IL-4 receptor or Janus kinase (JAK) inhibitors (such as

Received: 29 June 2024
Accepted: 24 October 2024
Published: 2 November 2024

Graphical Abstract

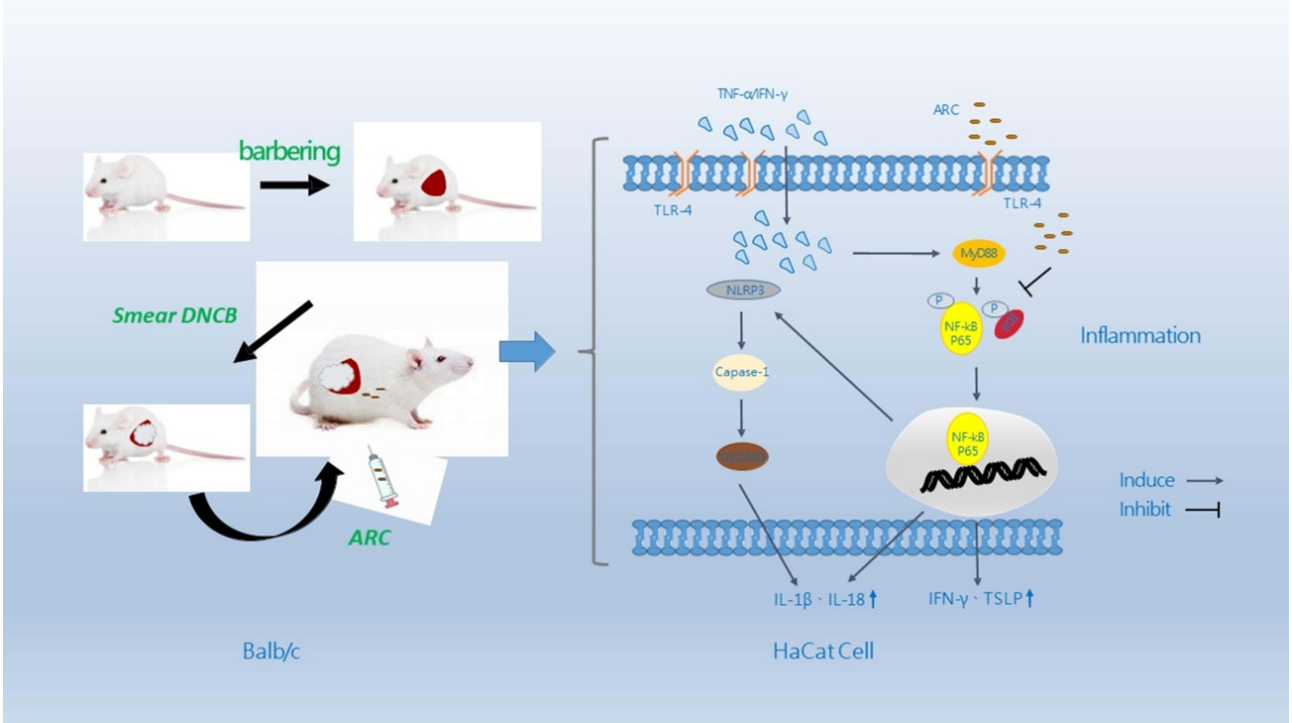

upadacitinib and baricitinib) have a curative effect for treating AD, but they can be costly and require long-term, intensive verification.[7] Therefore, it is essential to find new drugs that can effectively relieve the symptoms of AD, possess long-term applicability, and have minimal adverse effects.

The immune response is a crucial factor throughout the development of AD. Specifically, Th2-type cells play a pivotal role in acute AD, while Th1-type cells exhibit an enhanced inflammatory response in chronic AD. Nuclear factor-κB (NF-κB) serves as a critical component in regulating the Th1/Th2 immune and inflammatory response.[8] Research has consistently indicated that TLR4, a key player in strengthening inflammation and immune responses, plays a critical role in the onset and progression of AD.[9] Moreover, it has been shown that the inflammatory molecule NLRP3 and pyroptosis are closely related to the induced inflammatory response in AD.[10] Therefore, inhibiting TLR4/NF-κB and pyroptosis may be effective targets for the treatment of AD.

Arctii (*Fructus arctii*) is the mature fruit of *Arctium lappa L.* from the Compositae family. It has garnered interest in traditional medicine as a frequently utilized herbal remedy and has demonstrated efficacy for the treatment of various ailments, including the treatment of pyrexia, dizziness, diabetes, toothache, furuncle, and alopecia.[11] Arctiin (ARC) is a lignan compound and has been identified as the primary active ingredient and marker compound in *Arctii*, as listed in the Chinese pharmacopoeia. It is abundantly present in *Arctium lappa L.* as well as in more than 38 plant species.[12] ARC exhibits diverse biological activities, including anti-inflammatory, anti-allergic, anti-cancer, anti-bacterial, anti-oxidant, and anti-platelet properties, and it can function as a calcium antagonist.[13] ARC is known to alleviate IgE-mediated passive skin allergic reactions and anaphylactic shock triggered by compound 48/80.[14] Studies have demonstrated that it has potent anti-inflammatory effects by inhibiting the NF-κB transport pathway and reducing the production of inflammatory mediators such as IL-6, IL-1β, and TNF-α.[15]

However, the impact of ARC on AD remains uncertain. Therefore, our study aimed to evaluate the effects of ARC on AD in Balb/c mice induced by DNCB and in HaCat cells stimulated by TNF-α and IFN-γ.

Materials and Methods

Arctiin

Arctiin was purchased from Beijing Solarbio Science&Technology Co.,Ltd., (Beijing, China), with High Performance Liquid Chromatography (HPLC) ≥98%, batch number: SA8440.

Animals

Balb/c mice (female, aged 6–8 weeks, 20±2g) were purchased from Huafukang Biotechnology Co. Ltd. (Beijing, China, RRID: IMSR_APB:4790). All mice were housed in stainless steel cages in a pathogen-free and strictly controlled environment (12h light/12h dark cycle; temperature: 22 ± 1 °C; humidity: 55 ± 5%). They were fed with food and water *ad libitum*. All research procedures were conducted in accordance with Guidelines for the Care and Use of Laboratory Animals issued by the National Institutes of Health and were approved by the Ethics Committee of China Medical University (2022PS1149K).

Induction of AD and Treatment

Before the experiment, all mice were kept for 1 week to adapt to the laboratory environment. A total of 24 mice were classified into four groups (n = 6 each): the control group, model group, arctiin group (25mg/kg, ARC group); positive control group (1mg/kg, dexamethasone, DEX group). After grouping by random number method, 24 mice were randomly divided into four groups: the control group, model group, arctiin group (25mg/kg, ARC group), and positive control group (1mg/kg, dexamethasone, DEX group). First, the mice were numbered 1–24, and 24 two-digit random numbers were generated by checking the random number version. After arranging the random numbers from small to large, the serial number R was obtained, and R = 1–6 was specified as control group, R = 7–12 was model group, R = 13–18 was arctiin group, and R = 19–24 was positive control group. An individual unconnected to the experiment was employed to represent AD symptoms in mice.

To induce AD-like skin lesions, 1% DNCB solution (dissolved with a mixture of acetone and olive oil) was applied onto the shaved dorsal skin of the mice with an approximate area of 2×2 cm^2. Mice were sensitized once on days 1 and 2, followed by the application of 0.5% DNCB solution every 2 days for a total of 9 times. For the control group, 200μL of vehicle (acetone: olive oil = 3:1) was applied on the shaved backs of mice. Beginning on the fourth day of the experiment, the mice in the ARC and DEX group were intraperitoneally administered with arctiin or dexamethasone, respectively. Mice in the control and DNCB group were treated with PBS of equal volume once every day for 17 days. Lesions on the back of the mice were photographed once a week, and the thickness of the back skin was measured with a vernier caliper. The mice were sacrificed on day 21 (Figure 1), and blood was collected. The dorsal skin was then

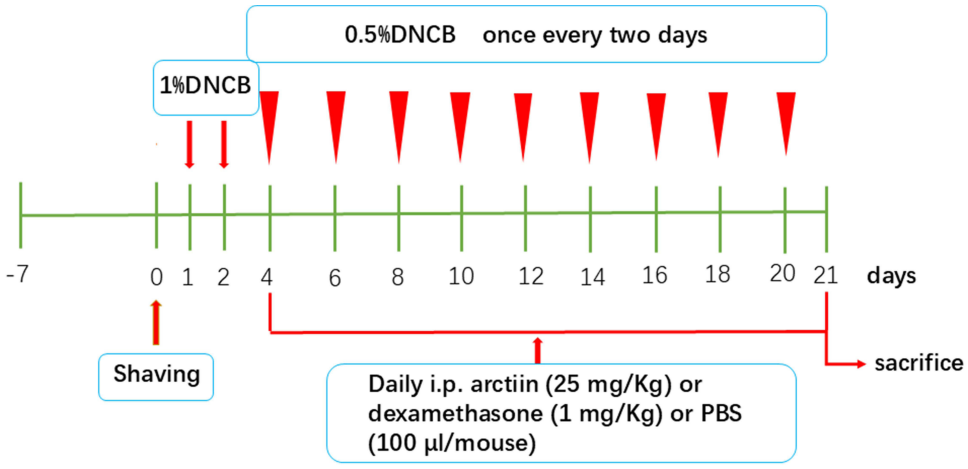

Figure 1 Schematic diagram of the animal experiment.

isolated, with part of it fixed in 4% paraformaldehyde for histological analysis and the remainder stored at −80 °C for subsequent studies.

Evaluation of the Severity of Skin Dermatitis and Dorsal Skin Thickness

The severity of dermatitis in the dorsal skin was evaluated once a week from Day0. Dorsal skin severity scores were recorded weekly for mice based on four skin symptoms (erythema, edema, dryness and ulceration). The scoring range indicators were 0 (none), 1 (mild), 2 (moderate) and 3 (severe). The sum of the individual scores was defined as the dermatitis score.[16]

A vernier caliper was utilized for measuring the thickness of the dorsal skin of the mouse. The tool was positioned on the midline of the dorsal skin and the measurement was automatically recorded.[17]

Measurement of Serum IgE

Blood samples were collected at the end of the experiment, and serum samples were obtained using a microcentrifuge (3000 rpm, 15min). Total serum level of IgE was measured using an ELISA assay kit (Elabscience, Wuhan, China), according to the manufacturer's instructions.

Histological Analysis

The mice were sacrificed at the end of the experiment, the dorsal skin tissue obtained from mice was fixed in 4% paraformaldehyde for 24h, and then embedded in paraffin. The embedded tissues were then sectioned at 3.5μm. We stained the sections with hematoxylin and eosin (H&E) and toluidine blue (TB) to observe the histological changes by measuring the thickness of the epidermis and the mast cell infiltration. The sections were photographed using an Olympus BX53 microscope (Olympus, Tokyo, Japan).

Immunohistochemistry

The sections were deparaffinized in graded alcohol and xylene and then washed with cold PBS. Antigen retrieval was performed with enzymatic antigen (Zhongshan Goldenbridge Biotechnology Co., Beijing, China) at 37 °C, 30 min. Next, the sections were treated using a histochemical kit (PV-9000, Zhongshan Goldenbridge Biotechnology Co., Beijing, China), according to the manufacturer's instructions. Specific anti-body anti-NLRP3 (1:100, Proteintech Group, United States, RRID: AB_10646484), anti-TLR4 (1:100; Cell Signaling Technology, RRID:AB_2924306), anti-NF-κB p65 (1:100; Cell Signaling Technology, RRID:AB_330561), anti-GSDMD (1:100; Proteintech, RRID:AB_10696319), anti-IL-1β (1:100; Cell Signaling Technology, RRID:AB_2715503) were then incubated with the sections overnight at 4 °C. The next day, the tissue sections were washed with PBS and then incubated with biotin-labeled goat anti-rabbit/mouse IgG polymer at 37°C, 30min. The sections were then stained using diaminobenzidine (DAB) and counterstained with hematoxylin for 1min. Dehydrated tissue sections were sealed and observed at ×400 magnification using optical microscopy (Eclipse Ci, Nikon, Chiyoda, Japan).

Cell Culture

Minimum Essential Medium (Procell Life Science&Technology Co.,Ltd. Wuhan, China) supplemented with 15% fetal bovine serum (Procell Co.,Ltd.) and 1% penicillin–streptomycin antibiotic (Procell Co.,Ltd.) was used to culture HaCaT cells (Procell Co.,Ltd., CVCL_0038). The cells were cultured maintained at 37°C in a humidified incubator containing 5% CO_2.

Cytotoxicity Assay

Cell viability assay was conducted using the Cell Counting Kit-8 (CCK-8) Assay (GK10001, GLPBIO, USA). HaCaT cells were seeded in 96-well plates (1×10^4 cells/sample). Following overnight stabilization, the cells were incubated in serum-free medium containing varying concentrations of ARC (0, 25, 50, 100, 200, and 400 μg/mL). After a 24-hour exposure to ARC, 10μL of CCK-8 solution was added to each well and further incubated for an additional hour. Then the cell viability was measured at 450nm absorbance using a Gen5 plate reader (BioTek, Winooski, United States).

Immunofluorescence Microscopy

The HaCaT cells were seeded onto coverslips in a 24-well plate, followed by pretreatment with ARC at a concentration of 400μg/mL. Three hours later, the cells were stimulated with TNF-α/IFN-γ at a concentration of 10ng/mL each for 24h. Subsequently the cells were fixed with 4% paraformaldehyde, and then incubated with NF-κB p65 antibodies at 4°C overnight (1:1000, Cell Signaling Technology, Inc., USA, RRID:AB_330561). The next day, the cells were further incubated with the anti-rabbit IgG (H + L) F (ab′)2 fragment (Alexa Fluor® 488 conjugate) (1:200; Proteintech) for 1h at room temperature. The nuclei were stained using 4,6-diamidino-2-phenylindole (DAPI) for 5min. Finally, the coverslips were observed and imaged using a confocal microscope (Olympus).

Western Blot

Cells or tissues were homogenized in RIPA buffer (Solarbio Life Science&Technology Co.,Ltd. Beijing, China) with 1 mm PMSF (Solarbio) and 1 mm phosphatase inhibitors (Solarbio). Subsequently, the lysates were centrifuged at 12,000rpm for 15min at 4°C to collect the supernatants. The protein concentrations were determined using the bicinchoninic acid (BCA) protein assay kit (Epizyme, Co.,Ltd. Shanghai, China). Equal amounts of protein were separated by sodium dodecyl sulfate polyacrylamide gel electrophoresis (10% SDS-PAGE) and then transferred to polyvinylidene fluoride (PVDF) membranes. The PVDF membrane was blocked with 5% skimmed milk or 3% bovine serum albumin (BSA) at 25 °C for 2h and then washed three times with Tris-buffered saline containing 0.1% Tween-20 (TBST). The membrane was subsequently incubated overnight with the following primary antibodies at 4°C: anti-TLR4 (1:1000; Cell Signaling Technology, RRID:AB_2924306), anti-MyD88 (1:2000; Proteintech, RRID:AB_2879236), anti-NF-κB p65 (1:1000; Cell Signaling Technology, RRID:AB_330561), anti-phosphorylated-NF-κB p65 (1:1000; Cell Signaling Technology, RRID: AB_2341216), anti-IκBα (1:1000; Proteintech, RRID:AB_2151423), anti-phosphorylated-IκBα (1:1000; Proteintech, RRID:AB_3073626), anti-NLRP3 (1:1000; Proteintech, RRID:AB_10646484), anti-ASC (1:1000; Proteintech, RRID: AB_2174862), anti-Caspase-1 (1:1000; Proteintech, RRID:AB_2935555), anti-GSDMD (1:1000; Proteintech, RRID: AB_10696319), anti-IL-1β (1:1000; Cell Signaling Technology, RRID:AB_2715503), anti-IL-18 (1:1000; Proteintech, RRID:AB_2123636), and anti-β-actin (1:1000; Proteintech, RRID:AB_10700003). The next day, the PVDF membranes were washed with TBST three times and then incubated with goat anti-rabbit/mouse IgG H&L (HRP) (1:10,000; Proteintech) at 25°C, 1h. After three washes with TBST, the bands were visualized using enhanced chemiluminescence (Millipore, United States), quantified using ImageJ software, and normalized against β-actin.

Quantitative Reverse Transcription Polymerase Chain Reaction (qRT-qPCR)

Total RNA was extracted from the cells or dorsal tissue using TRIZOL reagent (Vazyme Biotech Co., Ltd., Nanjing, China). We then utilized HiScript II Q RT SuperMix for qPCR (Vazyme Biotech Co., Ltd.) to reverse-transcribe 1 μg RNA into cDNA.

Real-time PCR was conducted using the SYBR Green mixture (Vazyme Biotech Co., Ltd. databas) with the Applied Biosystems 7500 Real-Time PCR System. The cycling conditions for amplification were executed as follows: step 1: 95 °C for 30s; step 2: 95 °C for 5 s, 40 cycles at 60 °C for 30s; step 3: 95 °C for 15s, 60 °C for 60s, and 95 °C for 15s. The target gene expression was quantified by the $2^{-\Delta\Delta CT}$ method, mRNA levels of genes were normalized to β-actin. The primers were purchased from Sangon, China (Table 1).

Molecular Docking

The molecular docking analysis is an effective method for investigating the atomic-level interaction between a protein and a small molecule.[18] In this study, we conducted molecular docking between arctiin and TLR4 using AutoDock Vina 4.0 to explore their binding mode. The 3D molecular model of arctiin (CID:100528) was obtained from PubChem database (https://pubchem.ncbi.nlm.nih.gov), while the three-dimensional structure of TLR4 (PBD ID:3FXI) was downloaded from Research Collaboratory for Structural Bioinformatics Protein Data Bank (http://www.rcsb.org/pdb/).The search grid of the TLR4 was identified as center_x: 21.383, center_y: −14.226, and center_z: 16.565 with dimensions

Table 1 Primer Sets for qRT-PCR

Gene	Oligonucleotide Primers Forward (5'- 3') Reverse (3'- 5')
Human GSDMD	GCCTCCACAACTTCCTGACAGATG GGTCTCCACCTCTGCCCGTAG
Human IL-1β	GGACAGGATATGGAGCAACAAGTGG TCATCTTTCAACACGCAGGACAGG
Human NLRP3	AGGGATGAGAGTGTTGTGTGAAACG GCTTCTGGTTGCTGCTGAGGAC
Human β-actin	CATGTACGTTGCTATCCAGGC CTCCTTAATGTCACGCACGAT
Mouse β-actin	GTGCTATGTTGCTCTAGACTTCG ATGCCACAGGATTCCATACC
Mouse ASC	GGACGGAGTGCTGGATGCTTTG CATCTTGTCTTGGCTGGTGGTCTC
Mouse Caspase-1	ATACAACCACTCGTACACGTCTTGC TCCTCCAGCAGCAACTTCATTTCTC
Mouse IL-18	CAAAGTGCCAGTGAACCCCAGAC ACAGAGAGGGTCACAGCCAGTC
Mouse TSLP	TATGAGTGGGACCAAAAGTACCGAGCTTGTCTCCTGAAAATCGAG
Mouse IFN-γ	GGGATTGAAGGTTAGGCTCTGGAGGTTTGATTCAGGCAGATGTT TTCAGCAACAGCAAGGCGAA CGCTTCCTGAGGCTGGATTC

size_x: 15, size_y: 15, and size_z: 15. The value of exhaustiveness was set to 50. The molecular docking results were generated using PyMoL 2.6 software.

Transmission Electron Microscope (TEM)

HaCaT cells were fixed with 2.5% glutaraldehyde at room temperature for 4h. The fixed cells were then embedded with 1% agarose blocks. The agarose blocks containing samples were fixed with 1% Ted Pella Inc in 0.1 M PB (pH 7.4) for 2h at room temperature and washed three times with distilled water, followed by gradient dehydration with 30%, 50%, 70%, 80%, and 95% ethanol for 20min each. The embedding models with resin and samples were moved into 65°C oven to polymerize for more than 48h. The resin blocks were then removed from the embedding models for standby application at room temperature. Then resin penetration and embedding as followed: Acetone:EMBed 812=1:1 for 2–4h at 37°C; Acetone:EMBed 812=1:2 overnight at 37°C; pure EMBed 812 for 5–8 h at 37°C. The pure EMBed 812 was poured into the embedding models and tissues were inserted, then kept in 37°C oven overnight. After that the embedding models with resin and samples were moved into 65°C oven to polymerize for more than 48h. Finally, the sections were sliced with an ultrathin microtome, stained with uranium for 8min, and photographed under a TEM (Tokyo, Japan).

Statistical Analysis

Statistical analysis was conducted using GraphPad Prism 10.0 and the results were presented as the mean ± standard deviation (SD). We used Shapiro–Wilk test to assess their normality. To analyze multiple groups with more than two, we performed a one-way analysis of variance, then post-hoc analysis using Bonferroni correction for normally distributed data and the Kruskal–Wallis test for non-normally distributed data, with P-value < 0.05 considering statistically significant.

Results

Effect of ARC on Atopic Dermatitis in Balb/c Mice Induced with DNCB

Effect of ARC on Atopic Skin Lesions in Balb/c Mice Induced with DNCB

To investigate the impact of ARC on AD, we induced dorsal skin inflammation in Balb/c mice with DNCB. Dexamethasone, typically employed in the management of immune-mediated skin conditions, served as a positive control to assess the impact of ARC on AD. During a span of three weeks, the mice were subjected to sensitization and challenge with 0.5–1% DNCB, resulting in AD-like lesions characterized by scratching, dryness, and lichenification. However, the administration of ARC and dexamethasone effectively alleviated these clinical symptoms (Figure 2A).

Furthermore, the dermatitis score index was significantly elevated in mice subjected to DNCB when compared to the control group. Nonetheless, ARC and dexamethasone remarkably suppressed these skin clinical scores (p<0.05) (Figure 2B and Table 2).

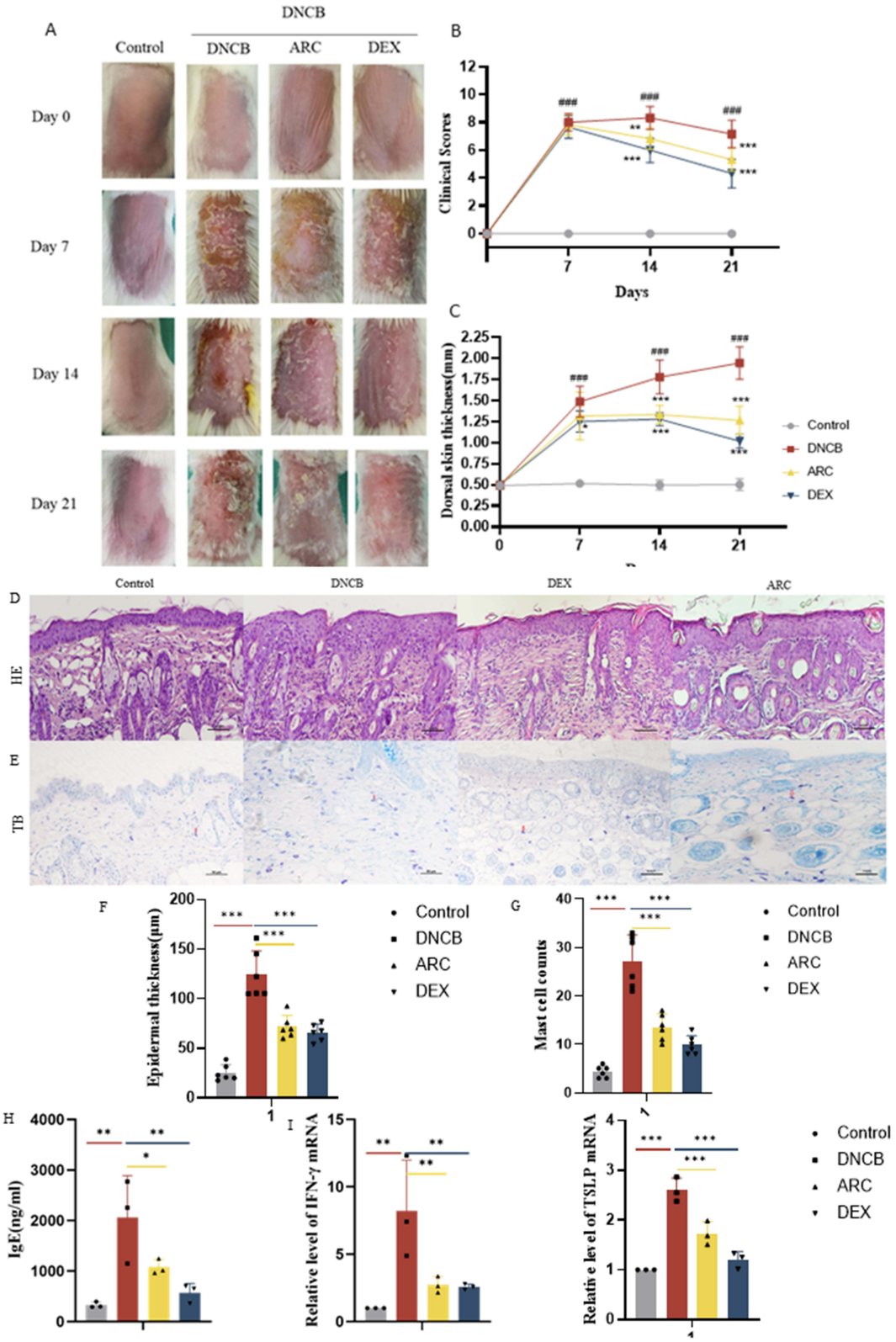

Figure 2 Effect of ARC on atopic skin lesions in Balb/c mice induced with DNCB: (**A**) Representative clinical features of skin lesions. (**B**) Clinical scores of skin lesion in different groups. (**C**) Dorsal skin thickness in different groups. (**D**) Histological analysis using H&E staining (200 × magnification). (**E**) Toluidine blue staining evaluation of mast cell infiltration in the skin. The red arrows indicate mast cells. (**F**) On H&E-stained slides, three random skin lesion sites were assessed using ImageJ to measure epidermal thickness (n = 6). (**G**) The number of mast cells in three randomly selected areas on slides stained with toluidine blue was counted to determine the mast cell infiltration in skin lesions (n = 6). (**H**) The levels of serum IgE in each group. (**I**) The levels of cytokines (IFN-γ, TSLP) in the dorsal skin. Data are shown as mean ± SD (n = 6). *$p < 0.05$, **$p < 0.01$, and ***$p < 0.001$ vs DNCB group; ### $p < 0.001$ vs normal control group.

Table 2 Dermatitis Score at Different Time (Mean ± SD, n = 6)

Time	Control	DNCB	ARC	DEX
Day0	0	0	0	0
Day7	0	8.000±0.3689	7.833±0.3689	7.667±0.3689
Day14	0	8.333±0.4116	6.833±0.4116	6.000±0.4116
Day21	0	7.167±0.4743	5.333±0.4743	4.333±0.4743

Skin thickness was assessed as an indicator of AD-like symptoms using a Vernier caliper. Mice treated with DNCB exhibited significantly thicker skin compared to the control group. However, treatment with ARC and dexamethasone led to a remarkable decrease in skin thickness ($p<0.05$) (Figure 2C and Table 3).

Histological analysis revealed no abnormalities in the skin of untreated mice. H&E staining (Figure 2D) demonstrated a significant increase in epidermal thickness in the DNCB-treated group compared to the control group, while treatment with ARC and dexamethasone effectively reduced DNCB-induced epidermal thickness (Figure 2F and Table 4). Toluidine blue staining (Figure 2E) revealed a marked increase in mast cell infiltration in the dermis of DNCB-treated mice, which was significantly reduced by treatment with ARC and dexamethasone ($p<0.05$) (Figure 2G and Table 5).

Effect of ARC on the Level of Serum IgE and Cytokines in the Dorsal Skin of DNCB-Induced Balb/c Mice

As hypersecretion of IgE has been identified as the predominant cause of AD,[19] the impact of ARC on serum IgE levels was analyzed using ELISA.

A drastic increase was observed in the DNCB group in comparison to normal control mice, which was notably inhibited by ARC and DEX (Figure 2H). Real-time PCR was utilized to evaluate the effects of ARC on the expression of inflammatory cytokines in the dorsal skin tissue of DNCB-induced AD-like mice. As illustrated in Figure 2I, the production of inflammatory cytokines (IFN-γ, TSLP) was significantly higher in the DNCB group relative to the normal control group. Nevertheless, ARC and DEX administration significantly reduced the DNCB-induced production of inflammatory cytokines.

Table 3 Skin Thickness at Different Times (Mean ± SD, n = 6)

Time	Control	DNCB	ARC	DEX
Day0	0.490±0.015	0.493±0.015	0.497±0.015	0.497±0.015
Day7	0.515±0.098	1.487±0.098	1.317±0.098	0.497±0.098
Day14	0.497±0.071	1.778±0.071	1.333±0.071	1.278±0.071
Day21	0.502±0.080	1.947±0.080	1.265±0.080	1.018±0.080

Table 4 Epidermal Thickness of H&E Staining (Mean ± SD, n = 6)

Group	Epidermal Thickness (μm)	t, *P* (vs Control group)	t, *P* (vs DNCB group)
Control	25.29±8.437		11.73, *P* <0.0001
DNCB	124.2±8.437	11.73, *P* <0.0001	
ARC	71.67±8.437	7.774, 0.0001	8.809, *P* <0.0001
DEX	66.02±8.437	6.826, 0.0005	9.757 *P* <0.0001

Table 5 Number of Mast Cells of Toluidine Blue Staining (Mean ± SD, n = 6)

Group	Number of Mast Cells	t, *P* (vs Control Group)	t, *P* (vs DNCB Group)
Control	4.333±1.873		17.24, *P* <0.0001
DNCB	27.17±1.873	17.24, *P* <0.0001	
ARC	13.50±1.873	6.921, 0.0005	10.32, *P* <0.0001
DEX	4.153±1.873	6.826, 0.0376	13.09, *P* <0.0001

Effect of ARC on TLR4/MyD88/NF-κB Signalling Pathway in Balb/c Mice Induced with DNCB

Gathering evidence continues to reveal the significant roles TLR4 plays in immune responses and inflammation. The activation of NF-κB and IκB can trigger the production of cytokines and chemokines, regulating and responding to inflammation.[20] To investigate the effect of ARC on TLR4/MyD88/NF-κB signalling pathway, firstly, we utilize immunohistochemical analysis to assess the protein expression of TLR4 and p65 in the dorsal skin. The outcomes demonstrate a notable rise in the count of positively-stained TLR4 and p65 cells in the DNCB group. However, ARC and DEX treatments exhibited a significant inhibition in the increased number of positively-stained cells induced by DNCB (Figure 3A). Furthermore, the expression of TLR4, MyD88, p65/p-p65, and IκBα/p-IκBα proteins was evaluated through Western blot. As shown in Figure 3B, repeated DNCB applications significantly increased the expression of TLR4, MyD88, p-p65, and p- IκBα. Thus, we verified that ARC and DEX administration notably suppressed the protein levels of TLR4, MyD88, as well as the phosphorylation of IκBα and NF-κB p65.

Effect of ARC on TLR4/MyD88/NF-κB Signalling Pathway in TNF-α/IFN-γ-Stimulated HaCaT Cells

TNF-α/IFN-γ stimulation was used to induce inflammation in HaCaT cells, representing an in vitro model for inflammatory skin diseases such as AD.[21] Firstly, we conducted the cell counting kit-8 (CCK-8) assay to evaluate the effects of ARC on cytotoxicity in HaCaT cells. Our results showed that 400μg/mL of ARC treatment for 24 hours did not cause obvious cytotoxicity to the HaCaT cells (Figure 4A). Therefore, we used concentrations 100, 200, 400μg/mL for ARC in subsequent experiments.

To further confirm the role of ARC on TLR4/MyD88/NF-κB signalling pathway, molecular docking experiments were conducted to investigate the interaction between arctiin and TLR4. Figure 4B and C illustrates the binding situation of ARC in the TLR4 pocket. Arctiin interacted with TLR4 through seven hydrogen bonds, and key interacting residues include Arg-264 (bond length: 1.8, 2.1 and 2.7 Å), Lys-362 (bond length: 2.2 Å), Thr-319 (bond length: 2.3 Å), and Leu-293 (bond lengths: 1.9 and 2.3 Å). Then we evaluated the protein expression of TLR4, MyD88, NF-κB p65/p- NF-κB p65, and IκBα/p- IκBα in HaCaT cells using Western blot analysis. In the model group stimulated by TNF-α/IFN-γ, the protein levels of TLR4, MyD88, p-p65, and p-IκBα were significantly higher than those in the normal control group. It was confirmed that pretreatment with ARC reduced the protein expression of TLR4, MyD88, and suppressed the phosphorylation of IκBα and p65. Moreover, the repressive impact of ARC was found to escalate commensurate with the concentration (Figure 4D). We also utilized an immunofluorescence microscope to assess the impact of ARC on p65 nuclear translocation in HaCat cells induced by TNF-α/IFN-γ. The outcomes revealed that TNF-α/IFN-γ induced the relocation of p65 from the cytoplasm to the nucleus, but ARC pretreatment effectively inhibited this nuclear translocation of p65 (Figure 4E). The results above demonstrated that ARC successfully suppressed the activation of the TLR4/MyD88/NF-κB signalling pathway in HaCaT cells stimulated by TNF-α/IFN-γ.

ARC Demonstrated Anti-Pyroptotic Effects by Suppressing the NLRP3/Caspase-1/GSDMD Cascade in Balb/c Mice Induced with DNCB

We used immunohistochemical staining to assess protein expression of NLRP3, GSDMD, and IL-1β in the dorsal skin. Our findings exhibited a significant elevation in the expression of the aforementioned proteins in the DNCB group as compared to the control group based on the number of positively-stained cells. Nevertheless, treatment with ARC and DEX led to a noteworthy suppression of expression ($p<0.05$) (Figure 5A). q-PCR analysis was utilized to evaluate mRNA expression of IL-18, caspase-1, and ASC, which revealed a significant increase in the DNCB group compared to the control group. Treatment with ARC and DEX resulted in a remarkable suppression of transcription ($p<0.05$) (Figure 5B–D).

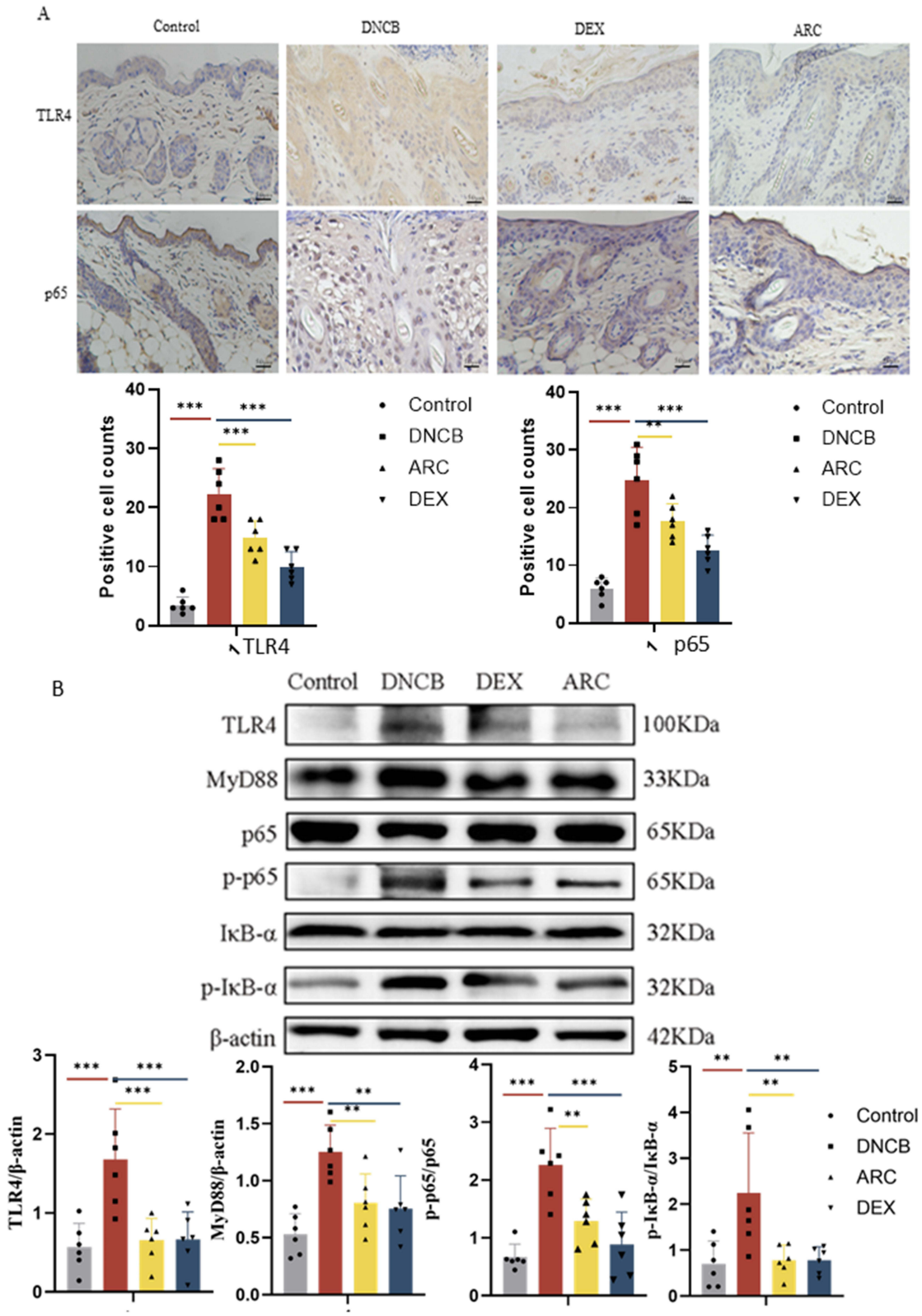

Figure 3 Effect of ARC on TLR4/MyD88/NF-κB signalling pathway in Balb/c mice induced with DNCB: (**A**) Changes in expression of the proteins TLR4 and NF-κB p65 in the dorsal skin were observed through immunohistochemistry. (**B**) Western blot to quantify protein TLR4, MyD88, NF-κB p65/p- NF-κB p65, and IκBα/p- IκBα in each group. Data are shown as mean ± SD (n=6). $^{**}p < 0.01$, and $^{***}p < 0.001$.

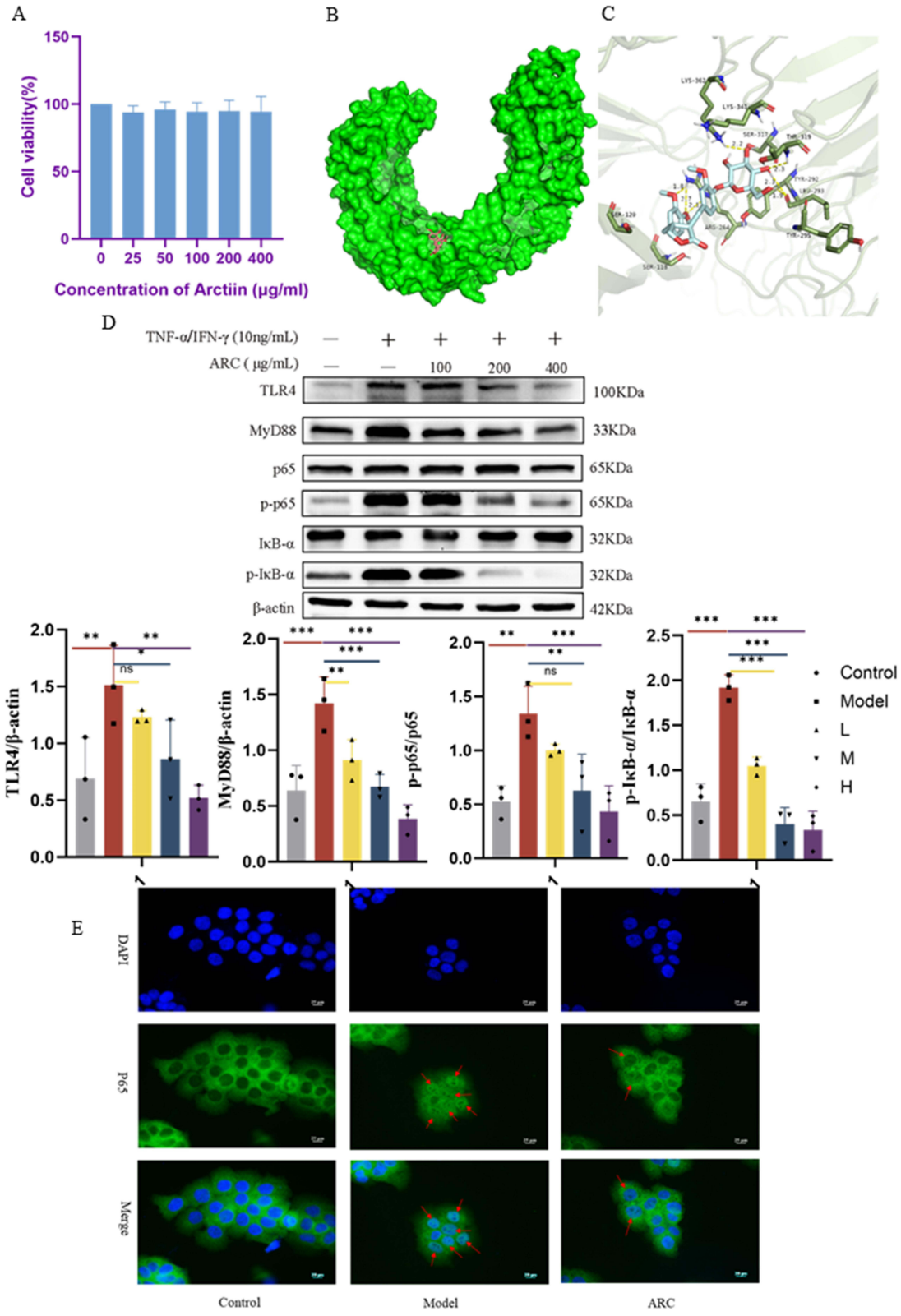

Figure 4 Effect of ARC on TLR4/MyD88/NF-κB signalling pathway in TNF-α/IFN-γ-Stimulated HaCaT Keratinocytes: (**A**) Cytotoxic effects of ARC in HaCaT cells. Cell viability of HaCaT cells under various concentrations (0, 25, 50, 100, 200, 400μg/mL) of ARC treatment for 24h. (**B**) Arctiin was docked into the binding pocket of TLR4, the total view. (**C**) the detailed view. (**D**) Protein levels of TLR4, MyD88, NF-κB p65/p- NF-κB p65, and IκBα/p- IκBα were measured by Western blot. HaCaT cells were pretreated with three different concentrations of ARC (100, 200, and 400μg/mL) for 3h, and then they were treated with TNF-α/IFN-γ (10 ng/mL) for 24h. (**E**) Translocation of p65 was measured by a fluorescent microscopy. Representative photomicrographs of (**A**) NF-κB p65 (green), (**B**) DAPI (blue), and (**C**) merged images (nuclear/cytosol) in HaCaT cells. HaCaT cells were pretreated with ARC (400μg/mL) for 3h, and then they were treated with TNF-α/IFN-γ (10ng/mL) for 24h. Data are shown as mean ± SD (n=3). *$p < 0.05$, **$p < 0.01$, and ***$p < 0.001$.

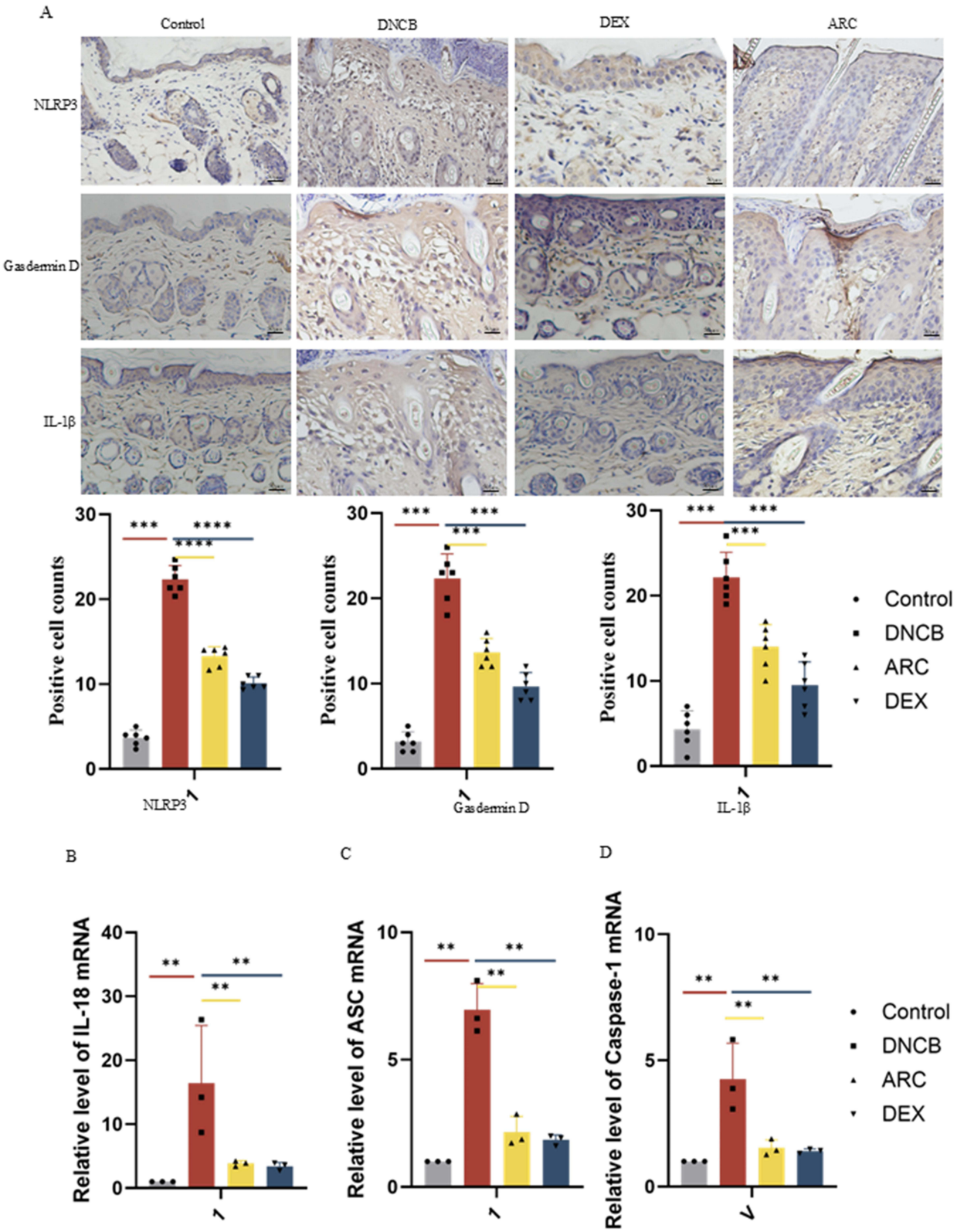

Figure 5 Effect of ARC on the NLRP3 inflammasome and pyroptosis in Balb/c mice induced with DNCB: (**A**) Changes in expression of the inflammation-related pyroptosis proteins NLRP3, IL–1β and GSDMD in the dorsal skin were observed through immunohistochemistry. (**B–D**) q-PCR measured relative mRNA expression of IL-18, caspase-1, and ASC in each group. Data are shown as mean ± SD (n = 3). $^{**}p < 0.01$, $^{***}p < 0.001$, and $^{****}p < 0.0001$.

ARC Demonstrated Anti-Pyroptotic Effects by Suppressing the NLRP3/Caspase-1/GSDMD Cascade in TNF-α/IFN-γ-Induced HaCaT Cells

To assess the anti-inflammatory mechanism of ARC, we further examined NLRP3 inflammasomes and pyroptosis in TNF-α/IFN-γ-Stimulated HaCaT cells via Western blot. In the model group stimulated with TNF-α/IFN-γ, the protein levels of NLRP3, GSDMD, caspase-1, ASC, IL-1β, and IL-18 were notably higher than those in the normal control group. Thus, we observed a gradual decrease of the expression levels pretreated with ARC (Figure 6A–G). This indicates that ARC positively impacted the increased expression of these proteins. Additionally, qPCR analysis of NLRP3, GSDMD, and IL-1β mRNA levels revealed that ARC mitigated the TNF-α/IFN-γ-induced increase in mRNA levels in HaCaT cells (Figure 6H–J). A transmission electron microscope (TEM) was employed to investigate inflammation-related pyroptosis by observing cellular structures. In the normal control group, the membrane structure was continuous and intact (Figure 6K). In the HaCaT cells stimulated by TNF-α/IFN-γ, partial nuclei were irregular in shape and reduced in size. Most of the mitochondrial structures appeared swollen, with discontinuous cristae and widening of cristae gaps. Many vacuoles were also evident (as shown by yellow arrows). A substantial number of autophagosomes were found, significantly more than the normal control group (marked by red arrows). As for the HaCaT cells pretreated with ARC, the nuclear morphology appeared relatively regular. Fewer mitochondrial cristae were widened, and most cristae were clearly visible.

Discussion

AD, as an intricate inflammatory disease, cannot be completely cured based on current clinical research.[22] Therefore, the primary management of AD includes ameliorating the clinical symptoms and achieving long-term disease control in accordance with treatment guidelines.[23] However, the long-term use of these inhibitors can potentially lead to a range of side effects, including localised skin atrophy from corticosteroids and a heightened risk of cancer from topical calcineurin inhibitors. Targeting the IL-4 receptor or using Janus kinase (JAK) inhibitors can be effective, but they can be costly and require long-term verification. Despite the continued use of phototherapy and conventional systemic immunosuppressive therapies for many years as frontline treatment options for moderate-to-severe cases, their limited efficacy and long-term toxicity have necessitated the exploration and development of new therapeutic interventions.[24]

Traditional medicine plays a critical role in the treatment and management of diseases.[25] Recently, there has been a growing interest in phytotherapeutic preparations for dermatology and cosmetology.[26] Furthermore, multiple human clinical studies have revealed that botanical extracts and herbal products can mitigate AD with no noticeable side effects. ARC, a glucoside of *artigenin*, is present in several species of *Asteraceae*, including *Forsythia viridissima, Centaurea imperialis*, and *Saussurea heteromalla*, and was originally isolated from *Arctium lappa L.*[15] As previously stated, ARC exhibits diverse biological properties, including strong antiallergic and anti-inflammatory effects. *Arctii* has traditionally been used to treat various skin problems, including sore throat and various diseases. Arctiin has proven to have significant inhibitory effects on the production of IgE in human myeloma U266 cells. In addition, the *arctii* extract plays a significant role in mitigating allergic responses by decreasing the production of histamine and pro-inflammatory cytokines including IL-1β, IL-6, IL-8, and TNF-α in mast cells. Furthermore, arctiin has been shown to inhibit IgE-mediated passive skin allergic reactions and anaphylactic shock induced by compound 48/80. This evidence suggests that arctiin has the potential to be a promising drug for the treatment of allergic inflammatory diseases. However, no previous study has examined its anti-AD effect; therefore, this study is the first to explore the therapeutic effects of ARC on AD.

This study utilized a DNCB-induced model of atopic dermatitis (AD) in BALB/c mice due to the fact that it exhibits characteristics that closely mimic human AD, including skin erosion, hemorrhage, epidermal hyperplasia, and histopathological features of mast cell infiltration. Additionally, the model exhibited increased levels of serum IgE and infiltration of inflammatory cells with thickened epidermis and dermis.[27] According to a previous study, approximately 80% of patients with AD have elevated serum IgE levels, which is one of the major signs of AD.[22] IgE has a strong affinity for the type I IgE-Fc receptor located on mast cells, which leads to the release of various inflammatory mediators.[28] This allergic reaction in AD leads to the increased infiltration of immune cells in the epidermis and dermis, resulting in skin thickening.[29,30] In addition, when T cell-mediated inflammatory cells penetrate the skin tissue, edema

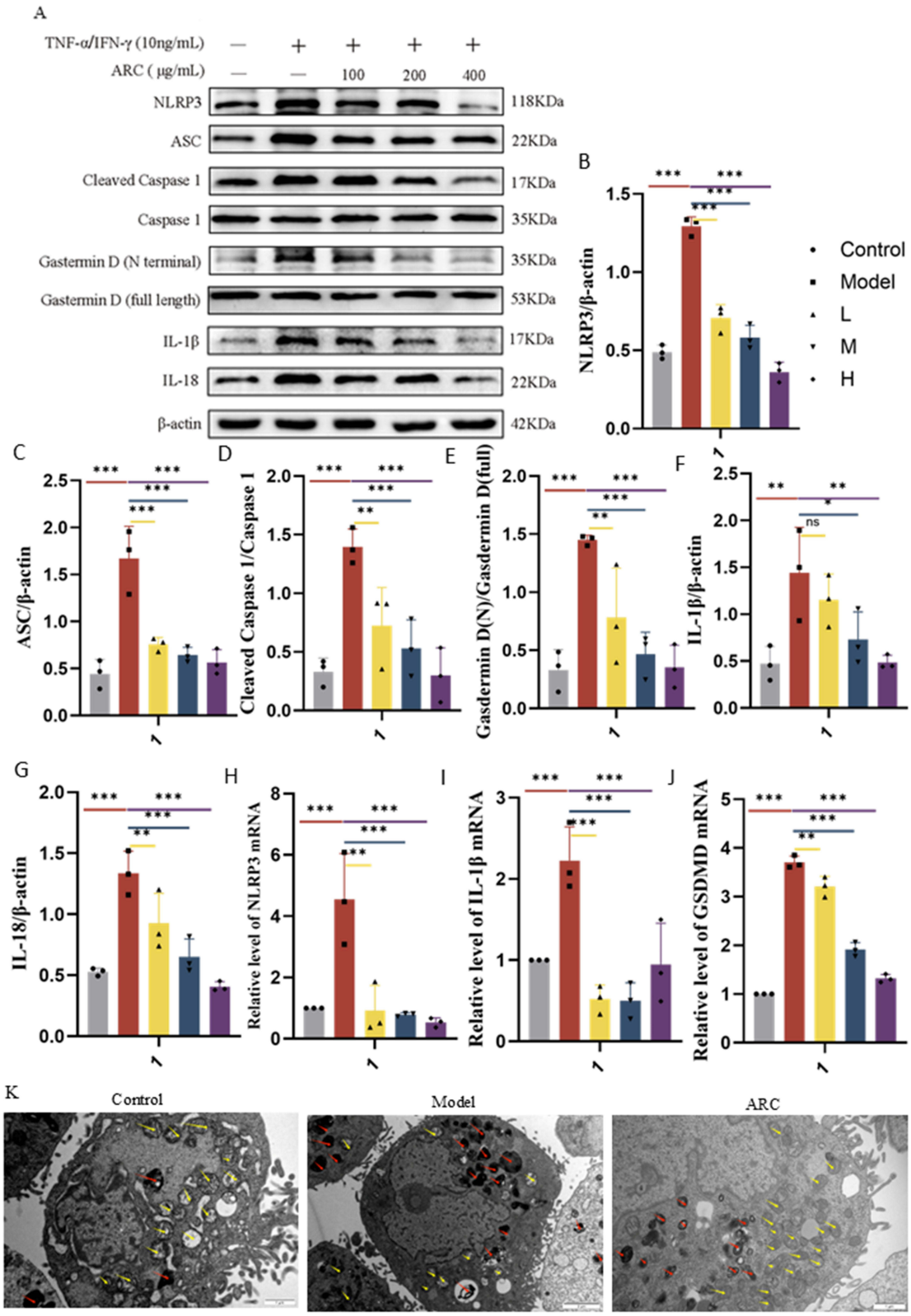

Figure 6 Effect of ARC on the NLRP3 inflammasome and pyroptosis in TNF-α/IFN-γ-Stimulated HaCaT Keratinocytes: (**A**–**G**) Western blot quantifying variations in protein expression related to pyroptosis in each group. (**H-J**) qPCR detecting the mRNA levels of NLRP3, GSDMD and IL-1β. (**K**) TEM images of cellular morphological changes. HaCaT cells were pretreated with ARC (400 μg/mL) for 3h, and then they were treated with TNF-α/IFN-γ (10 ng/mL) for 24h. Data are shown as mean ± SD (n=3). *p < 0.05, **p < 0.01, and ***p < 0.001.

and thickening occur, which further increase the thickness of the epidermis and dermis.[31] In this study, periodic external application of DNCB to the back skin of mice induced AD-like symptoms, such as erythema and lichenoid transformation, and the epidermis was significantly thickened, with obvious mast cell infiltration, and the serum total IgE levels were significantly increased. After ARC treatment, the dermatitis manifestations were significantly alleviated, the dermatitis score and thickness of the back skin were reduced, and mast cell infiltration was inhibited. At the same time, ARC lowered the serum IgE levels. These results indicate that ARC effectively alleviates AD symptoms in mice.

The immune response plays a crucial role in the pathogenesis of AD. Th2 cells are considered to be the key players in the acute phase of AD, and the cytokine TSLP promotes the Th2 immune response.[32] This leads to a chronic Th2 inflammatory response and stimulation of the sensory neurons, which ultimately induces the itching symptom.[8]

As symptoms worsen, the Th1 cytokines increase, further escalating the inflammatory response.[33] IFN-γ, a Th1 cytokine, is responsible for promoting Fas-mediated keratinocyte apoptosis, and it is a key factor in the development of eczema and dermatitis.[34] Our findings revealed that the mRNA levels of TSLP and IFN-γ were significantly suppressed by ARC treatment in AD mice, thus indicating that ARC has a potential therapeutic effect in mitigating inflammation by reducing the transcription of Th1 and Th2 proinflammatory cytokines.

In patients with AD, the expression of TLR4 gradually increases from the basal to the upper layer of the spinous layer. Furthermore, regardless of disease severity, the level of TLR4 expression in the peripheral blood mononuclear cells of patients with AD is higher than that of healthy individuals.[35] To date, animal and clinical studies have confirmed the importance of TLR4 in the occurrence and development of AD as both an inflammatory response amplifier[9] and an immune response module.[36] Except for TLR3, all TLRs on keratinocytes signal via the myeloid differentiation primary response protein 88 (MyD88).[37] TLR4 induces IFN-β (a MyD88-independent pathway) and induces an inflammatory response.[38] In the MyD88 pathway, TLR4 triggers the MyD88 signaling pathway, rapidly activating NF-κB and promoting the release of inflammatory cytokines.[39] NF-κB is a crucial transcription factor in inflammatory skin diseases that can serve as a valuable biomarker for monitoring the efficacy of treatment methods for conditions such as AD.[40] The increase and activation of NF-κB play a critical role in mediating the production of numerous cytokines, including IL-1β, and TNF-α, which contribute to the inflammatory response and exacerbation of AD.[41] Typically, NF-κB remains bound to IκBα in the cytoplasm; however, certain stimuli such as TNF-α/IFN-γ can induce the phosphorylation of IκBα, which separates NF-κB and IκBα. This allows NF-κB to translocate into the nucleus, activate the target gene,[42] and induce the release of inflammatory cytokines,[43] thereby perpetuating or intensifying the associated inflammatory response. In addition, in response to bacterial pathogen-associated molecular patterns (PAMPs), mast cells (MCs) activated by TLRs, such as TLR2 and TLR4, can trigger immediate degranulation in case of IgE-crosslinked FcεRI receptors.[9] Therefore, the TLR4/MyD88/NF-κB pathway is one of the key targets of AD therapy.

To accurately investigate the role of ARC in AD treatment, we performed molecular docking experiments to assess the binding of ARC and TLR4. ARC was found to bind tightly to the pocket of TLR4 in a compact conformation. One of the aryl groups of ARC was situated within the hydrophobic pocket of TLR4, surrounded by stable hydrophobic structures that were formed by the residues Arg-264, Lys-362, Thr-319, and Leu-293. Notably, seven hydrogen bonds were observed between ARC and TLR4, specifically with the residues Arg-264 (bond lengths of 1.8, 2.1, and 2.7), Lys-362 (bond length of 2.2), Thr-319 (bond length of 2.3), and Leu-293 (bond lengths of 1.9 and 2.7), which facilitated the anchorage of ARC at the TLR4 binding site. Furthermore, our findings revealed a remarkable increase in the protein expression of TLR4 and MyD88 in AD mice and HaCaT cells. In this study, we also observed the enhanced phosphorylation of p65 and IκBα in AD mice and HaCaT cells. Moreover, immunofluorescence microscopy analysis revealed a notable increase in p65 nuclear translocation. Nevertheless, ARC resulted in a significant reduction in TLR4 and MyD88 protein levels and p65 phosphorylation, as well as the inhibition of p65 nuclear translocation and TLR4/MyD88/NF-κB signaling pathway activation.

Specifically, IL-1β plays a significant role in the pathogenesis of inflammation-mediated skin disorders, such as AD.[44] In this study, it was observed that the DNCB group had elevated levels of IL-1β. However, ARC intervention significantly suppressed the protein levels of IL-1β. Thus, we further explored the possible mechanism of this phenomenon.

Pyroptosis is a proinflammatory form of programmed cell death that is characterized by the activation of the NLRP3 signaling pathway, formation of lethal pores, and release of proinflammatory factors.[45] It has previously been demonstrated that the inflammatory molecule NLRP3 and pyroptosis are intricately linked to the inflammatory response in AD.[10,46] NLRP3 recruits pro-Caspase-1 with the help of ASC, and Caspase-1 activation is triggered by the inflammasome assembly,[47] which subsequently cleaves Gasdermin D (GSDMD), leading to the formation of lethal pores and release of proinflammatory factors.[48] In addition, activated Caspase-1 cleaves and activates the precursors of IL-1β, and when IL-18 is released by cells, it triggers an inflammatory response.[49] Moreover, NLRP3 and ASC are crucial in antigen (Ag)-induced degranulation of mast cells (MCs) that have been allergized by IgE. MCs lacking NLRP3 or ASC failed to generate granulosomes. Furthermore, IgE-Ag-elicited anaphylaxis was effectively obstructed by a specific NLRP3 inhibitor.[50] Therefore, the inhibition of NLRP3 inflammasome activation and pyroptosis may be a critical target for the treatment of AD. In this study, it was observed that the DNCB group had elevated levels of NLRP3, GSDMD, and IL-1β proteins, as well as increased mRNA levels of ASC, Caspase-1, and IL-18. However, ARC intervention significantly suppressed the protein and mRNA levels of these markers. We further performed protein expression analysis of NLRP3, ASC, Caspase-1, GSDMD, IL-1β, and IL-18 in an AD cellular model. The results revealed a notable increase in their protein expressions in the model group, which were significantly reduced by pretreatment with ARC. In addition, we used transmission electron microscopy to observe alterations in the cellular microstructure, which further verified the anti-pyroptosis effect of ARC. These findings indicate that ARC effectively suppressed the activation of the NLRP3/Caspase-1/GSDMD signaling pathway, thereby reducing pyroptosis in AD.

Based on the in vivo and in vitro study findings, it is hypothesized that ARC has the potential to mitigate the inflammatory response and pyroptosis associated with AD by inhibiting the activation of the TLR4/MyD88/NF-κB and NLRP3/Caspase-1/GSDMD signaling pathways.

While the findings from our study provide valuable insights, they do have limitations. One important consideration is the fact that although DNCB is a commonly used compound for inducing in vivo models of AD, transcriptome analysis suggests that such models show around 40% homology to human AD. This finding may limit the generalizability of the conclusions drawn from our study to humans.

Conclusion

This is the first study to investigate the impact of ARC on AD. ARC effectively relieved the AD symptoms induced in mice with DNCB, reduced skin thickness, mast cell infiltration in the skin tissue, and total serum IgE levels. In both the in vivo and in vitro AD models, ARC inhibited the activation of the TLR4/MyD88/NF-κB and NLRP3/Caspase-1/GSDMD signaling pathways. Taken together, these results indicate that ARC has the potential to be an alternative treatment for AD, providing a new therapeutic target at the molecular level and contributing to the worldwide reduction of AD and quality of life enhancement for those afflicted.

Acknowledgments

This research was funded by the scientific research project: Study on the Mechanism of IL-37 Restoring the Skin Barrier Function of Atopic Dermatitis Based on Autophagy Regulation (Grant No. JYTMS20230095).

Disclosure

All the authors of this manuscript declare that they have no conflict of interest.

References

1. Nutten S. Atopic dermatitis: global epidemiology and risk factors. *Ann Nutr Metab*. 2015;66(Suppl 1):8–16. doi:10.1159/000370220
2. Langan SM, Irvine AD, Weidinger S. Atopic dermatitis. *Lancet*. 2020;396(10247):345–360. doi:10.1016/S0140-6736(20)31286-1
3. Müller S, Witte F, Ständer S. Pruritus in atopic dermatitis-comparative evaluation of novel treatment approaches. *Dermatologie*. 2022;73(7):538–549. doi:10.1007/s00105-022-05011-7
4. Xue Y, Bao W, Zhou J, et al. Global burden, incidence and disability-adjusted life-years for dermatitis: a systematic analysis combined with socioeconomic development status, 1990-2019. *Front Cell Infect Microbiol*. 2022;12:861053. doi:10.3389/fcimb.2022.861053
5. Bieber TA-O. Atopic dermatitis: an expanding therapeutic pipeline for a complex disease. *Nat Rev Drug Discov*. 2022;21(1):21–40. doi:10.1038/s41573-021-00266-6

6. Kleinman E, Laborada J, Metterle L, Eichenfield LF. What's new in topicals for atopic dermatitis? *Am J Clin Dermatol*. 2022;23(5):595–603. doi:10.1007/s40257-022-00712-0
7. Wan H, Jia H, Xia TA-O, Zhang D. Comparative efficacy and safety of abrocitinib, baricitinib, and upadacitinib for moderate-to-severe atopic dermatitis: a network meta-analysis. *Dermatol Ther*. 2022;35(9):e15636. doi:10.1111/dth.15636
8. Girolomoni G, Pastore S. The role of keratinocytes in the pathogenesis of atopic dermatitis. *J Am Acad Dermatol*. 2001;45(1 Suppl):S25–8. doi:10.1067/mjd.2001.117021
9. Molteni M, Gemma S, Rossetti CA-O. The role of toll-like receptor 4 in infectious and noninfectious inflammation. *Mediators Inflammation*. 2016;2016:6978936. doi:10.1155/2016/6978936
10. Zhang D, Li Y, Du C, et al. Evidence of pyroptosis and ferroptosis extensively involved in autoimmune diseases at the single-cell transcriptome level. *J Transl Med*. 2022;20(1):363. doi:10.1186/s12967-022-03566-6
11. Li Y, Wang Q, Wei HC, et al. Fructus arctii: an overview on its traditional uses, pharmacology and phytochemistry. *J Pharm Pharmacol*. 2022;74(3):321–336. doi:10.1093/jpp/rgab140
12. Gao Q, Yang M, Zuo Z. Overview of the anti-inflammatory effects, pharmacokinetic properties and clinical efficacies of arctigenin and arctiin from Arctium lappa L. *Acta Pharmacol Sin*. 2018;39(5):787–801. doi:10.1038/aps.2018.32
13. Wang W, Pan Q, Fau - Han X-Y, et al. Simultaneous determination of arctiin and its metabolites in rat urine and feces by HPLC. *Fitoterapia*. 2013;86:6–12. doi:10.1016/j.fitote.2013.01.016
14. Kee JY, Hong SA-O. Inhibition of mast cell-mediated allergic responses by arctii fructus extracts and its main compound arctigenin. *Journal of Agricultural and Food Chemistry*. 2017;65(43):9443–9452. doi:10.1021/acs.jafc.7b02965
15. Rolnik AA-O, Olas BA-O. The plants of the Asteraceae family as agents in the protection of human health. *Int J Mol Sci*. 2021;22(6):3009. doi:10.3390/ijms22063009
16. Leung DY, Hirsch Rl Fau - Schneider L, Schneider L, et al. Thymopentin therapy reduces the clinical severity of atopic dermatitis. *J allergy Clin Immunol*. 1990;85(5):927–933. doi:10.1016/0091-6749(90)90079-J
17. Wang L, Xian YF, Loo SKF, et al. Baicalin ameliorates 2,4-dinitrochlorobenzene-induced atopic dermatitis-like skin lesions in mice through modulating skin barrier function, gut microbiota and JAK/STAT pathway. *Bioorg Chem*. 2022;119:105538. doi:10.1016/j.bioorg.2021.105538
18. Meng XY, Zhang Hx Fau - Mezei M, Mezei M, Fau - Cui M, Cui M. Molecular docking: a powerful approach for structure-based drug discovery. *Curr Comput-Aided Drug Des*. 2011;7(2):146–157. doi:10.2174/157340911795677602
19. Park G, Moon BC, Ryu SM, Kim WJ, Lim HA-O. Cicadidae periostracum attenuates atopic dermatitis symptoms and pathology via the regulation of NLRP3 inflammasome activation. *Oxid Med Cell Longev*. 2021;2021(1):8878153. doi:10.1155/2021/8878153
20. Baeuerle PA, Baltimore D. I kappa B: a specific inhibitor of the NF-kappa B transcription factor. *Science*. 1988;242(4878):540–546. doi:10.1126/science.3140380
21. Tsai YC, Chang HH, Chou SC, et al. Evaluation of the anti-atopic dermatitis effects of α-boswellic acid on Tnf-α/Ifn-γ-stimulated hacat cells and DNCB-induced BALB/c mice. *Int J Mol Sci*. 2022;23(17):9863. doi:10.3390/ijms23179863
22. Weidinger S, Novak N. Atopic dermatitis [J]. *Lancet*. 2016;387(10023):1109–1122. doi:10.1016/S0140-6736(15)00149-X
23. Kim KA-O, Kim SA-O, Mony TJ, et al. Moringa concanensis L. alleviates DNCB-induced atopic dermatitis-like symptoms by inhibiting NLRP3 inflammasome-mediated IL-1β in BALB/c mice. *Pharmaceuticals*. 2022;15(10):1217. doi:10.3390/ph15101217
24. Alvarenga JA-O, Bieber TA-O, Torres TA-O. Emerging biologic therapies for the treatment of atopic dermatitis. *Drugs*. 2024;4:1179–1950.
25. Chew YA-O, Khor MA, Xu Z, et al. Cassia alata, Coriandrum sativum, Curcuma longa and Azadirachta indica: food ingredients as complementary and alternative therapies for atopic dermatitis-a comprehensive review. *Molecules*. 2022;27(17):5475. doi:10.3390/molecules27175475
26. Melnyk N, Vlasova I, Skowrońska WA-O, Bazylko AA-O, Piwowarski JP, Granica SA-O. Current knowledge on interactions of plant materials traditionally used in skin diseases in Poland and Ukraine with human skin microbiota. *Int J Mol Sci*. 2022;23(17):9644. doi:10.3390/ijms23179644
27. Yan SH, Chen YA-O, Huang ZQ, et al. Acupoint autohemotherapy attenuates DNCB-induced atopic dermatitis and activates regulatory T cells in BALB/c mice. *J Inflamm Res*. 2024;17:2839–2850. doi:10.2147/JIR.S454325
28. Werfel T, Allam JP, Biedermann T, et al. Cellular and molecular immunologic mechanisms in patients with atopic dermatitis. *J Allergy Clin Immunol*. 2016;138(2):336–349. doi:10.1016/j.jaci.2016.06.010
29. Hong S-W, Kim M-R, Lee E-Y. Extracellular vesicles derived from staphylococcus aureus induce atopic dermatitis-like skin inflammation. *Allergy*. 2011;66(3):351–359. doi:10.1111/j.1398-9995.2010.02483.x
30. Kim BE, Leung DYM. Significance of skin barrier dysfunction in atopic dermatitis. *Allergy Asthma Immunol Res*. 2018;10(3):207–215. doi:10.4168/aair.2018.10.3.207
31. Karuppagounder V, Arumugam S, Thandavarayan RA, et al. Tannic acid modulates NFκB signaling pathway and skin inflammation in NC/Nga mice through PPARγ expression. *Cytokine*. 2015;76(2):206–213. doi:10.1016/j.cyto.2015.05.016
32. Walker JA, McKenzie ANJ. T(H)2 cell development and function. *Nat Rev Immunol*. 2018;18(2):121–133. doi:10.1038/nri.2017.118
33. Oyoshi MK, He R, Fau - Kumar L, et al. Cellular and molecular mechanisms in atopic dermatitis. *Adv immun*. 2009;102:135–226. doi:10.1016/S0065-2776(09)01203-6
34. Trautmann A, Akdis M, Fau - kleemann D, et al. T cell-mediated Fas-induced keratinocyte apoptosis plays a key pathogenetic role in eczematous dermatitis. *J Clin Invest*. 2000;106(1):25–35. doi:10.1172/JCI9199
35. Shi J, He L, Tao R, et al. TLR4 polymorphisms as potential predictors of atopic dermatitis in Chinese Han children. *J Clin Lab Analysis*. 2022;36(5):e24385. doi:10.1002/jcla.24385
36. Lin L, Xie M, Chen X, et al. Toll-like receptor 4 attenuates a murine model of atopic dermatitis through inhibition of langerin-positive DCs migration. *Exp Dermatol*. 2018;27(9):1015–1022. doi:10.1111/exd.13698
37. Brandt EB, Gibson Am Fau - Bass S, Bass S, et al. Exacerbation of allergen-induced eczema in TLR4- and TRIF-deficient mice. *J Immunol*. 2013;191(7):3519–3525. doi:10.4049/jimmunol.1300789
38. Lin C, Wang H, Zhang M, et al. TLR4 biased small molecule modulators. *Pharmacol Ther*. 2021;228:107918. doi:10.1016/j.pharmthera.2021.107918
39. Guo BJ, Liu Z, Ding MY, et al. Andrographolide derivative ameliorates dextran sulfate sodium-induced experimental colitis in mice. *Biochem Pharmacol*. 2019;163:416–424. doi:10.1016/j.bcp.2019.03.019
40. Min GY, Kim TI, Kim JH, Cho WK, Yang JH, Ma JY. Inhibitory effect of isatis tinctoria L. water extract on DNCB-induced atopic dermatitis in BALB/c mice and HaCaT cells. *ChinMed*. 2022;17(1):66. doi:10.1186/s13020-022-00624-5

41. Jeong NH, Lee S, Choi YA, Song KS, Kim SA-O. Inhibitory effects of euscaphic acid in the atopic dermatitis model by reducing skin inflammation and intense pruritus. *Inflammation*. 2022;45(4):1680–1691. doi:10.1007/s10753-022-01652-x
42. Lee JH, Dong L, Noh HM, et al. Inhibitory effects of donkey hide gelatin on DNCB-induced atopic dermatitis in NC/Nga Mice. *Front Pharmacol*. 2022;13:896450. doi:10.3389/fphar.2022.896450
43. Hong SA-O, Kim EY, Lim SE, Kim JH, Sohn Y, Jung HA-O. Dendrobium nobile Lindley administration attenuates atopic dermatitis-like lesions by modulating immune cells. *Int J Mol Sci*. 2022;23(8):4470. doi:10.3390/ijms23084470
44. Xiao Y, Xu W, Su WA-O. NLRP3 inflammasome: a likely target for the treatment of allergic diseases. *Clin Exp Immunol*. 2018;48(9):1080–1091. doi:10.1111/cea.13190
45. Zeng X, Liu D, Huo X, Wu Y, Liu C, Sun Q. Pyroptosis in NLRP3 inflammasome-related atherosclerosis. *Cell Stress*. 2022;6(10):79–88. doi:10.15698/cst2022.10.272
46. Zheng JA-O, Yao L, Zhou Y, et al. A novel function of NLRP3 independent of inflammasome as a key transcription factor of IL-33 in epithelial cells of atopic dermatitis. *Cell Death Dis*. 2021;12(10):871. doi:10.1038/s41419-021-04159-9
47. Ma Y, Jiang J, Gao Y, et al. Research progress of the relationship between pyroptosis and disease. *Am J Transl Res*. 2018;10(7):2213–2219.
48. Newton KA-O, Dixit VA-O, Kayagaki NA-O. Dying cells fan the flames of inflammation. *Science*. 2021;374(6571):1076–1080. doi:10.1126/science.abi5934
49. Joly S, Sutterwala FS. Fungal pathogen recognition by the NLRP3 inflammasome. *Virulence*. 2010;1(4):276–280. doi:10.4161/viru.1.4.11482
50. Mencarelli A, Bist PA-O, Choi HA-O, Khameneh HA-O, Mortellaro AA-O, Abraham SA-O. Anaphylactic degranulation by mast cells requires the mobilization of inflammasome components. *Nat Immunol*. 2024;25(4):693–702. doi:10.1038/s41590-024-01788-y